Non-Fermi Liquid Behavior Induced by Resonant Diquark-pair Scattering in Heated Quark Matter

Masakiyo Kitazawa,[1,2] Teiji Kunihiro,[1] and Yukio Nemoto[3]

[1] *Yukawa Institute for Theoretical Physics, Kyoto University, Kyoto 606-8502, Japan*
[2] *Department of Physics, Kyoto University, Kyoto 606-8502, Japan*
[3] *Department of Physics, Nagoya University, Nagoya, 464-8602 Japan*

(Dated: February 2, 2008)

We show how the quasiparticle picture of quarks changes near but above the critical temperature T_c of the color-superconducting phase transition in the heated quark matter. We demonstrate that a non-Fermi liquid behavior of the matter develops drastically when the diquark coupling constant is increased owing to the coupling of the quark with the pairing soft mode: We clarify that the depression and eventually the appearance of a gap structure in the spectral function as well as the anomalous quark dispersion relation of the quark can be understood in terms of the *resonant scattering* between the incident quark and a particle near the Fermi surface to make the pairing soft mode.

PACS numbers: 25.75.Nq, 74.40.+k, 12.38.Aw, 11.15.Ex

I. INTRODUCTION

The recent data in the RHIC experiment suggest that the matter created by the RHIC seems to be a strongly coupled system with possible quasi-bound hadrons contained[1, 2]. Furthermore some lattice calculations, though in the quenched approximation, are consistent with the possible view that heavy-quark bound systems such as J/ψ survive the deconfinement transition at finite temperature T[3]. These developments have a possibility to change drastically the simple picture of the QGP phase that the system is composed of almost free quasi-particles, although such nontrivial properties of the QGP phase that it may contain quasi-hadronic excitations had been suggested earlier[4, 5].

In the present Letter, we shall argue that the *dense* quark matter at relatively low temperature can have also non-trivial properties, i.e., a *non*-Fermi liquid ones, if the system is close to the critical temperature T_c of the color-superconducting phase transition [6, 7] on a rather generic ground.

First we notice that the low energy effective models of QCD show that the diquark gap at zero temperature may become as large as $\Delta \sim 100$MeV[8, 9] at lower densities such as those corresponding to $\mu \simeq 400$MeV with μ being the baryon-number chemical potential of the quark. Accordingly, the ratio $r_\xi \equiv \Delta/\mu$, which is a measure of the ratio of the inter-particle distance to the pair coherence length, may become as large as 0.2 to 0.3. This value is much larger than those in the metal superconductors, i.e., $r_\xi \simeq 0.001$, which account for the validity of the mean-field approximation a lá BCS theory for the electric superconductors. Thus one sees that large fluctuations of the diquark-pair are expected, which may invalidate the mean-field approximation, in the color superconductors[10, 11].

In fact, our previous work with the fixed pairing coupling showed [12, 13] that there exists the precursory soft mode composed of the diquark-pair field even well above T_c. One of the remarkable points there was that the coupling of the quark with the soft mode not only modifies the quark dispersion relation but also causes a *depression* of the quark spectral function around the Fermi energy; the depression was so large that a "pseudogap" is formed in the density of states (DOS) of the quark even with the small diquark coupling that was employed.

The above finding is interesting because they suggest that the properties of quarks at T above but close to T_c are altered from the typical Fermi-liquid to the non-Fermi liquid ones owing to the coupling to the precursory fluctuations of the diquark-pair field. The mechanism to cause such a non-Fermi liquid behavior, however, might not have been clarified enough in the previous work. The purpose of the present Letter is to elucidate the mechanism to realize such a non-Fermi liquid behavior and argue that it is a generic feature of the heated quark matter in the vicinity of T_c of the color superconductivity.

For this purpose, we examine what happens in the quark properties in detail if the pairing fluctuations become stronger by increasing the diquark coupling constant G_C; we remark that the limiting case can often clarify physics. Incidentally it may be noticed that G_C indeed could have other values than that in the previous work without any contradiction with other principles and phenomenology. We calculate the dispersion relation and the spectral function of the quark in the T-matrix approximation[12, 13, 14].

We shall demonstrate the following for the first time: (1) The quark dispersion relation is so largely modified with the increasing G_C that it becomes seemingly multiple-valued around the Fermi surface near but above T_c in the strong coupling regime. (2) The quark spectral function gets to have a developed gap-like structure rather than a depression near but above T_c for the larger G_C. We shall clarify that the above non-Fermi liquid behaviors can be nicely understood in terms of the *resonant scattering*[15, 16] between the quark and a particle near the Fermi surface to make the pairing soft mode.

II. BRIEF SUMMARY OF FORMULATION

To describe a system at relatively low T and ρ, it is appropriate to adopt a low-energy effective theory of QCD [17, 18]. Here, we consider the two-flavor quark matter in the chiral limit with the four-Fermi quark-quark interaction[19]

$$\mathcal{L}_C = G_C \sum_A (\bar{\psi} i\gamma_5 \tau_2 \lambda_A C \bar{\psi}^T)(\psi^T C i\gamma_5 \tau_2 \lambda_A \psi), \qquad (1)$$

where $C = i\gamma_2\gamma_0$ is the charge conjugation operator, and τ_2 and λ_A denote the antisymmetric flavor $SU(2)_f$ and color $SU(3)_c$ matrices, respectively. The quark chemical potentials μ of each flavor and color are taken to be the same[13]. We introduce the three momentum cutoff $\Lambda =$ 650MeV[18]. As for the diquark coupling constant G_C, we vary it in the range $3.11\text{GeV}^{-2} < G_C < 4.35\text{GeV}^{-2}$, which is the similar range used in the references[8, 9, 17, 18].

In order to see the quasiparticle picture of the quarks, we examine the spectral function ρ_0 and the dispersion relation of the quark $\omega = \omega_-(\boldsymbol{k})$. The following formulation is essentially a recapitulation of that given in [13].

The spectral function ρ_0 is given by the imaginary part of the retarded Green function $G^R(\boldsymbol{k},\omega)$ as

$$\rho_0(\boldsymbol{k},\omega) = -\frac{1}{4\pi}\text{Tr}[\gamma^0 \text{Im} G^R(\boldsymbol{k},\omega)]. \qquad (2)$$

The Green function $G^R(\boldsymbol{k},\omega)$ is decomposed into the quark and anti-quark parts;

$$\begin{aligned} G^R(\boldsymbol{k},\omega) &= (G^R_-(\boldsymbol{k},\omega)\Lambda_-(\boldsymbol{k}) + G^R_+(\boldsymbol{k},\omega)\Lambda_+(\boldsymbol{k}))\gamma^0 \\ &= \frac{\Lambda_-(\boldsymbol{k})\gamma^0}{R_-(\boldsymbol{k},\omega)+i\eta} + \frac{\Lambda_+(\boldsymbol{k})\gamma^0}{R_+(\boldsymbol{k},\omega)+i\eta}, \end{aligned} \qquad (3)$$

with the projection operators $\Lambda_\mp(\boldsymbol{k}) = (1 \pm \gamma^0 \boldsymbol{\gamma}\cdot\hat{\boldsymbol{k}})/2$. The dispersion relations of the quarks and anti-quarks $\omega = \omega_\mp(\boldsymbol{k})$ are defined by the equations

$$\text{Re} R_\mp(\boldsymbol{k},\omega) = 0, \qquad (4)$$

respectively. A remark is in order here: Because $\omega_\mp(\boldsymbol{k})$ is merely the solution of the real part but not the whole part of the inverse of the Green function $R_\mp(\boldsymbol{k},\omega_\mp)$, $\omega_\mp(\boldsymbol{k})$ may not correspond to the peak position of the spectral function and hence also may not represent physical excitations when the imaginary part of the Green function is large.

Our point in the calculation of the quark Green function $G^R(\boldsymbol{k},\omega)$ lies in incorporating the diquark-pair fluctuations in the quark self-energy in the T-matrix approximation[12, 13, 14] as is diagrammatically shown in Fig. 1; all the possible anomalous behaviors of the results will originate from the fact that the pair fluctuations actually form the soft mode of the color-superconducting phase transition.

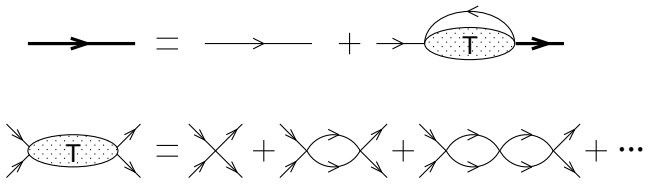

FIG. 1: Feynman diagrams representing the quark Green function in the T-matrix approximation. The thin lines represent the free propagator $\mathcal{G}_0$, while the bold ones the full propagator $\mathcal{G}$.

In the Matsubara formalism, the self-energy of quarks in the imaginary time $\tilde{\Sigma}(\boldsymbol{k},\omega_n)$ is given by

$$\begin{aligned} &\tilde{\Sigma}(\boldsymbol{p},\omega_n) \\ &\quad = 8T\sum_m \int \frac{d^3\boldsymbol{k}}{(2\pi)^3}\tilde{\Xi}(\boldsymbol{p}+\boldsymbol{k},\omega_n+\omega'_m)\mathcal{G}_0(\boldsymbol{k},\omega'_m), \end{aligned} \qquad (5)$$

with $\omega_n = (2n+1)\pi T$ being the Matsubara frequency for fermions and $\mathcal{G}_0(\boldsymbol{k},\omega_n) = [(i\omega_n+\mu)\gamma^0 - \boldsymbol{k}\cdot\boldsymbol{\gamma}]^{-1}$ being the free quark propagator. The T-matrix for the quark-quark scattering $\tilde{\Xi}(\boldsymbol{k},\nu_n)$ reads

$$\tilde{\Xi}(\boldsymbol{k},\nu_n) = -G_C \frac{1}{1+G_C\mathcal{Q}(\boldsymbol{k},\nu_n)}, \qquad (6)$$

with the lowest order polarization function $\mathcal{Q}(\boldsymbol{k},\nu_n)$[13] and $\nu_n = 2n\pi T$. The T-matrix in the real time $\Xi^R(\boldsymbol{k},\omega) \equiv \tilde{\Xi}(\boldsymbol{k},\nu_n)|_{i\nu_n\to\omega+i\eta}$ has all the information about properties of the pair fluctuations. In particular, the dynamical structure factor

$$S(\boldsymbol{k},\omega) = -\frac{\text{Im}\ \Xi^R(\boldsymbol{k},\omega)}{2\pi G_C^2(1-\text{e}^{-\omega/T})}, \qquad (7)$$

represents the excitation probability of the pair field for each ω and $\boldsymbol{k}$ at finite T. It has a prominent peak at the origin near T_c according to the softening of the pair fluctuations.

The analytic continuation of $\tilde{\Sigma}(\boldsymbol{k},\omega_n)$ to the real axis from the upper-half complex-energy plane gives the self-energy in the real time $\Sigma^R(\boldsymbol{k},\omega) = \tilde{\Sigma}(\boldsymbol{k},\omega_n)|_{i\omega_n\to\omega+i\eta}$. Using the projection operators $\Lambda_\mp(\boldsymbol{k})$, the self-energy is decomposed into the quark and anti-quark parts $\Sigma_\mp(\boldsymbol{k},\omega) = \text{Tr}[\Sigma^R(\boldsymbol{k},\omega)\Lambda_\mp(\boldsymbol{k})\gamma^0]/2$, and $R_\mp(\boldsymbol{k},\omega)$ in Eq. (3) is now found to be $R_\mp(\boldsymbol{k},\omega) = \omega + \mu \mp k - \Sigma_\mp(\boldsymbol{k},\omega)$. Notice that $\rho_0(\boldsymbol{k},\omega)$ around the Fermi energy is given almost solely by the quark part G^R_-, and hence the corresponding part of the self-energy $\Sigma_-(\boldsymbol{k},\omega)$ is responsible for the quasiparticle properties of the quark near the Fermi surface. For later convenience, we rewrite the explicit form of $\text{Im}\Sigma_-(\boldsymbol{k},\omega)$ given in [13] slightly using $S(\boldsymbol{k},\omega)$;

$$\begin{aligned} &\text{Im}\Sigma_-(\boldsymbol{k},\omega) \\ &\quad = \frac{\pi G_C^2}{2}\int \frac{d^3\boldsymbol{q}}{(2\pi)^3} S(\boldsymbol{k}+\boldsymbol{q},\omega+E_q-\mu)\left\{1-\frac{\hat{\boldsymbol{k}}\cdot\boldsymbol{q}}{E_q}\right\} \end{aligned}$$

$$\times \left[(1 - \mathrm{e}^{-(\omega+E_q-\mu)/T}) \tanh \frac{E_q - \mu}{2T} \right.$$
$$\left. -(1 + \mathrm{e}^{-(\omega+E_q-\mu)/T}) \right] + (E_q \to -E_q), \quad (8)$$

with $E_q = |\boldsymbol{q}|$.

III. NON-FERMI LIQUID BEHAVIOR AND RESONANT SCATTERING

In this section, we show the spectral function $\rho_0(\boldsymbol{k}, \omega)$ and the dispersion relation of quarks $\omega = \omega_-(\boldsymbol{k})$ to see the quasiparticle picture of quarks. As was promised in the Introduction, we vary the diquark coupling constant G_C for a fixed $\varepsilon \equiv (T - T_c)/T_c = 0.01$.

The upper panels of Fig. 2 show the spectral function $\rho_0(\boldsymbol{k}, \omega)$ for $\mu = 400$MeV and $\varepsilon = 0.01$ with several values of G_C, while the lower panels the dispersion relation $\omega = \omega_-(\boldsymbol{k})$ together with the contour map of the strength of $\rho_0(\boldsymbol{k}, \omega)$ represented by the shadow.

The figures in the far left show those with the same G_C ($T_c = 40.04$ MeV) as those presented in Refs. [12, 13] for comparison: Although the detailed properties of them are given in the previous paper[13], the essential points may be summarized as follows; (1) There appears a depression of the quasiparticle peak in the spectral function $\rho_0(\boldsymbol{k}, \omega)$ around the Fermi energy $\omega = 0$. This means that the life-time of the quasiparticles near the Fermi surface becomes short owing to the pair fluctuations. (2) The quark dispersion $\omega_-(\boldsymbol{k})$ shows a rapid increase around the Fermi momentum.

In the middle and the far right panels of Fig. 2, G_C is increased 1.2 and 1.4 times larger than that in the far left panels, respectively; correspondingly, $T_c \to 59.82$ and 80.11 MeV. One sees from the figures that as G_C is increased, the depression of $\rho_0(\boldsymbol{k}, \omega)$ around the Fermi energy becomes more significant, and the quasiparticle peaks tend to be so completely depressed that the profile of $\rho_0(\boldsymbol{k}, \omega)$ around the Fermi momentum may be characterized more properly with the term of a gap-like structure rather than with a depression. In the lower panels, $\omega_-(\boldsymbol{k})$ around the Fermi-momentum shows more rapid increase for larger G_C, and eventually becomes triple-valued. Here one should notice that $\omega_-(\boldsymbol{k})$ does not necessarily represent the real excitation spectrum since it is only a zero of the real part of the inverse of the Green function, as is noticed before. Indeed, one sees only two quasiparticle peaks in $\rho_0(\boldsymbol{k}, \omega)$ for $k = k_F$, corresponding to the first and third solutions of $\omega_-(\boldsymbol{k})$. The reason of the disappearance of the middle solution of $\omega_-(\boldsymbol{k})$ in $\rho_0(\boldsymbol{k}, \omega)$ will be given later.

The above features of $\rho_0(\boldsymbol{k}, \omega)$ and $\omega_-(\boldsymbol{k})$ can be understood by the behavior of the quark self-energy $\Sigma_-(\boldsymbol{k}, \omega)$. In Fig. 3, we show the imaginary and real parts of $\Sigma_-(\boldsymbol{k}, \omega)$ in the upper and lower panels, respectively, at $k = k_F$ for several G_C corresponding to each panel of Fig. 2. For each G_C, one sees a peak of $|\mathrm{Im}\Sigma_-(\boldsymbol{k}, \omega)|$ and a rapid increase of $\mathrm{Re}\Sigma_-(\boldsymbol{k}, \omega)$ around the Fermi energy $\omega = 0$, which is more significant for larger G_C. In fact, the size of G_C is important for the enhancement of $\Sigma_-(\boldsymbol{k}, \omega)$ because of the factor G_C^2 in Eq. (8) [22]. We notice that the behavior of $\mathrm{Re}\Sigma_-(\boldsymbol{k}, \omega)$ can be understood by the growth of $|\mathrm{Im}\Sigma_-(\boldsymbol{k}, \omega)|$ and the Kramers-Kronig relation

$$\mathrm{Re}\Sigma_-(\boldsymbol{k}, \omega) = -\frac{1}{\pi} \mathrm{P} \int d\omega' \mathrm{Im}\Sigma_-(\boldsymbol{k}, \omega')/(\omega - \omega'). \quad (9)$$

The peculiar behavior of $\omega_-(\boldsymbol{k})$ can be understood as follows. First, recall that $\omega_-(\boldsymbol{k})$ at $k = k_F$ is the solution of $\mathrm{Re}\ R_-(\boldsymbol{k}_F, \omega) = \omega - \mathrm{Re}\ \Sigma_-(\boldsymbol{k}_F, \omega) = 0$. Accordingly, the solutions $\omega_-(\boldsymbol{k}_F)$ are given graphically by the crossing points of $\mathrm{Re}\Sigma_-(\boldsymbol{k}_F, \omega)$ and ω denoted by the straight dash-dotted line in the lower panel of Fig. 3. One sees how there eventually appear the three solutions of $\omega_-(\boldsymbol{k}_F)$ for large G_C, as mentioned before. A remark is in order here: The group velocity as defined by $v_g = d\omega_-(k)/dk$ is seemingly larger than the speed of light near $\omega_-(k) = 0$. However, it corresponds to the peak position of the imaginary part of the self-energy $|\mathrm{Im}\Sigma_-(\boldsymbol{k}, \omega)|$, which means that the excitations around the origin have a quite large damping rate, and hence there does not appear a peak in the spectral function. The solution near $\omega = 0$ thus does not represent a physical excitation spectrum of the quasiparticle.

Now let us discuss the mechanism to realize the gap-like structure in the quark spectrum in Fig. 2. Due to the softening of the diquark-pair fluctuations near T_c [12, 13], a particle near the Fermi energy is scattered by the soft mode and creates a hole, while a hole can create a particle by absorbing the soft mode as shown in Fig. 4(a). We remark that the hole must be also created near the Fermi surface because of the energy conservation[13]. More intuitively, the incident particle and a particle near the Fermi surface, which may be within the Fermi sea or thermally excited one, make a resonant scattering to form the pairing soft mode and vice versa. This resonating processes which are only effective around the Fermi surface induce a virtual mixing between the particles and holes, i.e. a (virtual) Bogoliubov transformation! In other words, because the particle and hole energies $\omega = k - \mu$ and $\omega = \mu - k$ cross at the Fermi energy as shown in Fig. 5, the mixing between the particles and holes leads to the level repulsion of the energy spectrum of the particle and hole, which makes the gap-like structure as shown in the right panels of Fig. 2. This mechanism which induces the gap-like structure owing to the *resonant scattering* to make the softening pairing mode is also known in the condensed matter physics [16].

We shall next show how the behavior of the quark spectrum can be nicely reproduced by quantifying the notion of the resonant scattering. As was seen above, the softening of the pair fluctuations near T_c is responsible for the resonant scattering to become effective. Since the softening is described as the enhancement of $S(\boldsymbol{k}, \omega)$ around the origin in the $\boldsymbol{k}$-ω plane, let us approximate the dy-

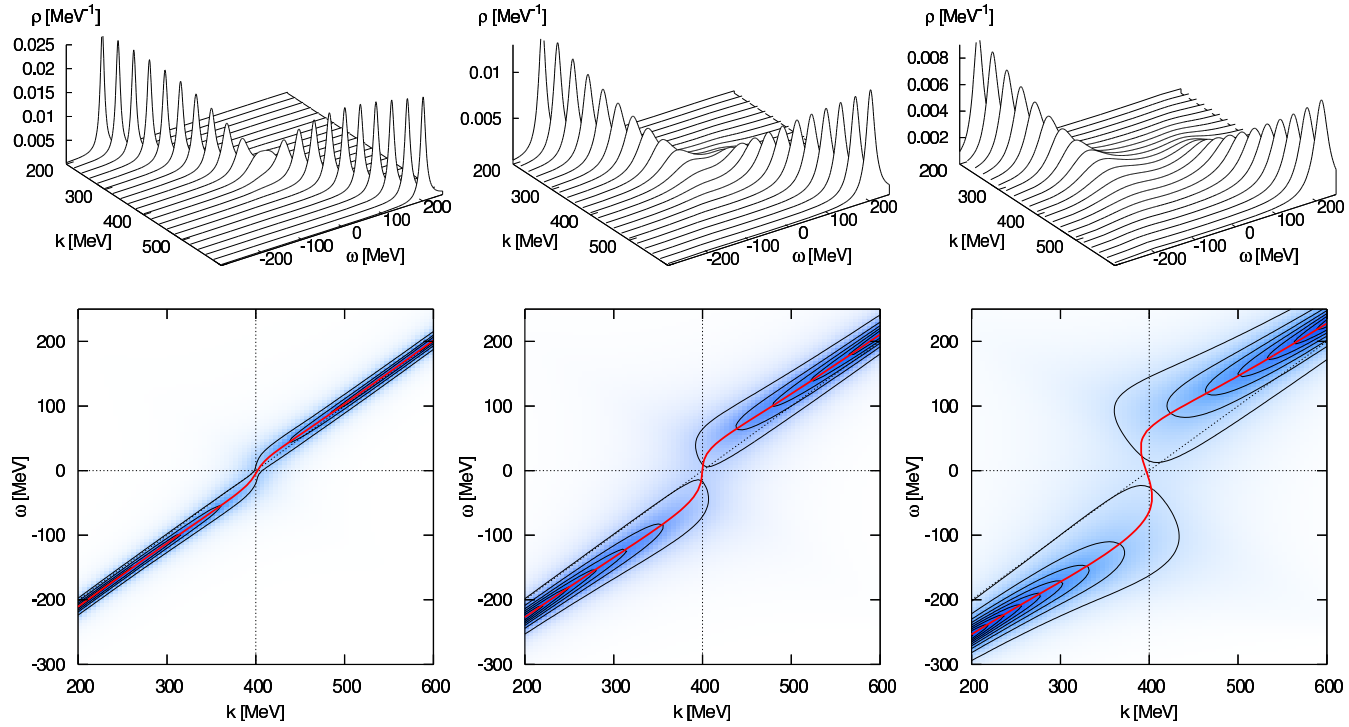

FIG. 2: The spectral function $\rho_0(\boldsymbol{k},\omega)$ (upper panels) and the dispersion relation of quarks $\omega = \omega_-(\boldsymbol{k})$ (lower panel) for $\mu = 400$MeV and $\varepsilon \equiv (T - T_c)/T_c = 0.01$. In the far left, middle and far right panels, the diquark coupling constant is taken $G_C = 3.11\text{GeV}^{-2}$, $3.73(= 3.11 \times 1.2)\text{GeV}^{-2}$ and $4.35(= 3.11 \times 1.4)\text{GeV}^{-2}$, respectively.

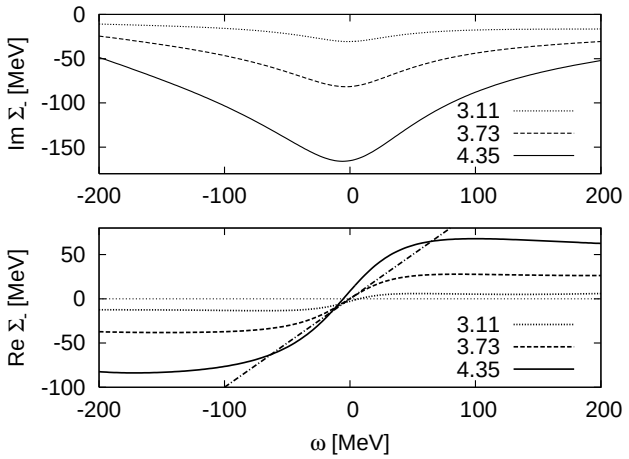

FIG. 3: The imaginary and real parts of the self-energy of quarks $\Sigma_-(\boldsymbol{k}_F,\omega)$ at $k_F = \mu = 400$MeV for $G_C = 3.11, 3.73$ and 4.35. As G_C is increased, the peak of $\text{Im}\Sigma_-(\boldsymbol{k}_F,\omega)$ as well as the increase of $\text{Re}\Sigma_-(\boldsymbol{k}_F,\omega)$ around the Fermi energy $\omega = 0$ becomes significant. The dash-dotted line in the bottom panel denotes $\omega = k - \mu$. For larger G_C, there exist three solutions of Re $R_-(\boldsymbol{k},\omega) = 0$, giving the multi-valued dispersion relation.

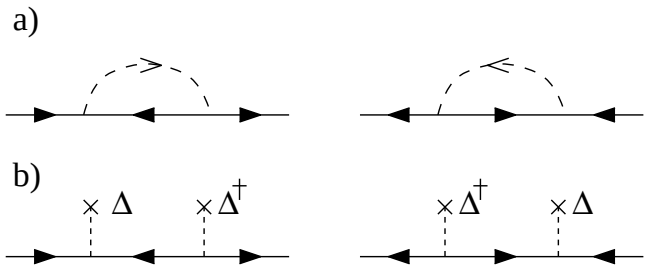

FIG. 4: (a) The self-energy of quarks above T_c. The dashed line denotes the collective mode of the pair fluctuations. The virtual mixing between the particles and holes is induced by the collective mode. (b) The self-energy in the BCS theory. The gap Δ induces the mixing.

namical structure factor with the delta function at the origin;

$$S(\boldsymbol{k},\omega) = \Delta^2 \frac{(2\pi)^4}{\pi G_C^2} \delta^{(3)}(\boldsymbol{k})\delta(\omega). \tag{10}$$

The meaning of the choice of the pre-factor containing a Δ in front of the delta functions will be clear later; Δ is to be related with the imaginary part of the T matrix Ξ and the boson distribution function [15, 16]. Needless to say, the dynamical structure factor above T_c in reality never vanishes in the whole ω-k plane nor takes the form of Eq. (10) even at $T = T_c$; the fluctuations with finite ω and k make a width of the quasiparticles. However,

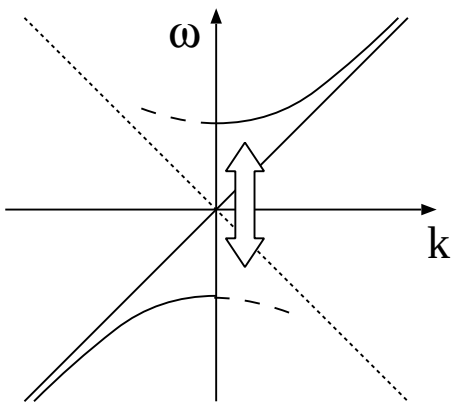

FIG. 5: The quasiparticle energy of quarks.

this simple treatment will be found to clearly illustrate that the peculiar behavior of the quark spectrum can be nicely accounted for by the resonant scattering.

A simple calculation with Eq. (8) leads to

$$\mathrm{Im}\Sigma_-(\boldsymbol{k},\omega) = -\pi\Delta^2\delta(\omega+|\boldsymbol{k}|-\mu), \tag{11}$$

$$\mathrm{Re}\Sigma_-(\boldsymbol{k},\omega) = \Delta^2\frac{1}{\omega+|\boldsymbol{k}|-\mu}. \tag{12}$$

Then, $R_-(\boldsymbol{k},\omega)=0$ gives real number quasiparticle energies

$$\omega_-(\boldsymbol{k}) = \pm\sqrt{(|\boldsymbol{k}|-\mu)^2+\Delta^2}, \tag{13}$$

which have the same form as that in the usual BCS theory with the energy gap Δ; notice that the quark propagator for the quarks which interact with the pairing mode with the dynamical structure factor Eq. (10) can be diagrammatically interpreted as Fig. 4(b), i.e., the quarks interacting with a static source of the pair field Δ.

IV. SUMMARY AND CONCLUDING REMARKS

In this Letter, motivated with the findings in our previous papers[12, 13], we have tried to elucidate generically that the precursory pairing soft mode modifies the quasiparticle picture of the quark so much that the heated quark matter would become a non-Fermi liquid in the vicinity of T_c of the color superconductivity. For this purpose, we have examined the changes of the quark properties in detail when the diquark coupling is increased. We have found that in the strong coupling regime the quark dispersion relation is modified so greatly that it becomes multiple-valued around the Fermi surface near but above T_c. The stronger coupling also changes the quark spectral function as to have a gap-like structure rather than a depression. We have shown that these non-Fermi liquid behaviors can be understood in terms of the resonant scattering between the incident particle and a particle around the Fermi energy to make the pairing soft mode.

Although the present work is based on a model calculation, the mechanism proposed here for realizing a non-Fermi liquid behavior of fermion systems can be model-independent. This is because the essential ingredient here is the scattering of a particle near Fermi surface to make the soft mode which is inherent to any second-order or weak first-order phase transition. It would be thus intriguing to explore the quasiparticle picture near the critical temperature of other phase transitions of QCD matter, including the *chiral* phase transition at finite temperature[20].

We should notice that there is another mechanism which causes a non-Fermi liquid behavior of ungapped quark matter: A resummed perturbation theory shows [21] that the coupling of the quark with unscreened long-range gauge (gluonic) fields gives rise to vanishing of both the residues of the quasiparticle excitations and the group velocity $v_g = dE/dp$ at the Fermi surface at small temperature without recourse to any phase transition. Notice that the vanishing group velocity implies the infinite density of states of quasiparticles, which is highly in contrast with our result, i.e., the pseudogap formation as a precursory phenomenon of the CSC at finite T. Although the perturbation theory adopted in [21] is only applicable for extremely high-density quark matter, it would be interesting to see how the non-Fermi liquid behaviors due to unscreened gluonic fields survive and compete with those owing to the soft mode of CSC at moderate density and temperature.

In this work, we have employed the non-selfconsistent T-matrix approximation which is essentially a linear approximation for the fluctuations. Nevertheless the results obtained in this approximation can be close to reality so long as $\varepsilon \equiv (T-T_c)/T_c$ is not so small as noted in [12, 13]; see [15]. In the present work, the strong fluctuations of the pair-field were induced with the varied G_C for fixed $\varepsilon = 0.01$. Similar results may be obtained for smaller ε but with a fixed G_C since the fluctuations diverge as ε goes to zero.

The situation, however, might not become so simple when the system may enter the Ginzburg region where the nonlinear fluctuation effects play an essential role and somewhat moderate behavior may be realized for the quark properties. A renormalization-group treatment, for instance, would be necessary to incorporate the nonlinear effects of the fluctuations, which is beyond the scope of the present work and left for future investigations.

M. K. is supported by Japan Society for the Promotion of Science for Young Scientists. T. Kunihiro is supported by Grant-in-Aide for Scientific Research by Monbu-Kagaku-sho (No. 14540263). Y. N. is supported by 21st Century COE Program of Nagoya University.

[1] K. Adcox *et al.* [PHENIX Collaboration], Nucl. Phys. A **757**, 184 (2005).

[2] E. V. Shuryak and I. Zahed, Phys. Rev. C **70**, 021901 (2004) ; Phys. Rev. D **70**, 054507 (2004) ; G. E. Brown, C. H. Lee, M. Rho and E. Shuryak, Nucl. Phys. A **740**, 171 (2004).

[3] T. Umeda, R. Katayama, O. Miyamura and H. Matsufuru, Int. J. Mod. Phys. **A16**, 2215 (2001); T. Umeda, K. Nomura and H. Matsufuru, Euro. Phys. J. **C39**S1, 16 (2005). M. Asakawa and T. Hatsuda, Phys. Rev. Lett. **92**, 012001 (2004); S. Datta, F. Karsch, P. Petreczky and I. Wetzorke, Phys. Rev. D **69**, 094507 (2004).

[4] T. Hatsuda and T. Kunihiro, Phys. Lett. B **145**, 7 (1984); Phys. Rev. Lett. **55** (1985) 158.

[5] C. DeTar, Phys. Rev. D **32**, 276 (1985).

[6] D. Bailin and A. Love, Phys. Rep. **107**, 325 (1984).

[7] K. Rajagopal and F. Wilczek, Chap. 35 in the Festschrift in honor of B.L. Ioffe, 'At the Frontier of Particle Physics / Handbook of QCD', M. Shifman, ed., (World Scientific), hep-ph/0011333.

[8] M. Alford, K. Rajagopal and F. Wilczek, Phys. Lett. **B422**, 247 (1998).

[9] R. Rapp, T. Schafer, E. Shuryak and M. Velkovsky, Phys. Rev. Lett. **81**, 53 (1998).

[10] M. Kitazawa, T. Koide, T. Kunihiro and Y. Nemoto, Phys. Rev. D **65**, 091504 (2002).

[11] D. N. Voskresensky, Phys. Rev. C **69**, 065209 (2004).

[12] M. Kitazawa, T. Koide, T. Kunihiro and Y. Nemoto, Phys. Rev. D **70**, 056003 (2004).

[13] M. Kitazawa, T. Koide, T. Kunihiro and Y. Nemoto, Prog. Theor. Phys. **114**, 117 (2005).

[14] L.P. Kadanoff and G. Baym, *Quantum statistical mechanics*, (W.A. Benjamin, 1962).

[15] See, reviews, Y. Yanase, T. Jujo, T. Nomura, H. Ikeda, T. Hotta and K. Yamada, Phys. Rep. **387**, 1 (2003), and references therein.

[16] B. Jankó, J. Maly and K. Levin, Phys. Rev. B **56**, R11407 (1997).

[17] J. Berges and K. Rajagopal, Nucl. Phys. **B538**, 215 (1999).

[18] T.M. Schwarz, S.P. Klevansky and G. Papp, Phys. Rev. C **60**, 055205 (1999).

[19] T. Hatsuda and T. Kunihiro, Phys. Rept. **247**, 221 (1994).

[20] M. Kitazawa, T. Kunihiro and Y. Nemoto, hep-ph/0510167.

[21] D. Boyanovsky and H. de Vega, Phys. Rev. D **63**, 034016 (2001).
The complete calculations were, however, presented in; T. Schaefer and K. Schwenzer, Phys. Rev. D **70**, 054007 (2004); A. Gerhold, A. Ipp, and A. Rebhan, Phys. Rev. D **70**, 105015 (2004); A. Gerhold and A. Rebhan, Phys. Rev. D **71**, 085010 (2005); A. Gerhold, hep-ph/0503279 and the references therein.
See also for the case of the nonrelativistic degenerate electron gas, T. Holstein, R. E. Norton and P. Pincus, Phys. Rev. B **8**, 2649 (1973).

[22] The dynamical structure factor $S(\boldsymbol{k}, \omega)$ around the origin for $\varepsilon = 0.01$ is not very sensitive to G_C in the range of G_C employed in this work, while the fluctuations for larger momentum become more significant as G_C is increased.